Catal Lett (2008) 126:218–223
DOI 10.1007/s10562-008-9682-3

Synthesis of the Ag^+-Bipyridine Complexes Anchored within MCM-41 and their Photocatalytic Reactivity for N_2O Reduction with CO

Haijun Chen · Satoru Kuranari · Masaya Matsuoka · Jinlong Zhang · Masakazu Anpo

Received: 11 March 2008 / Accepted: 16 September 2008 / Published online: 7 October 2008

Abstract Bipyridine derivatives were covalently anchored on the surface of the mesopores of MCM-41 porous material and the further introduction of Ag^+ ions led to the formation of Ag^+ bipyridine complexes by the chelation of the Ag^+ ions with the bipyridine units. The successful covalent immobilization of the bipyridine derivatives as well as the Ag^+ bipyridine complexes has been confirmed by various spectroscopic investigations such as FT-IR, UV-vis, and XPS analyses. It was found that the anchored bipyridine derivatives on the surface of MCM-41 prevent the reduction and agglomeration of the Ag^+ species even after evacuation treatment at 573 K. Thus, the anchored Ag^+ ions chelated with the bipyridine units inside the mesopores of MCM-41 were observed to exhibit photocatalytic reactivity for N_2O reduction with CO.

Keywords Ag photocatalyst · Ag bipyridine complex · The reduction of N_2O

1 Introduction

The removal of nitrous oxide (N_2O) from the exhaust of internal combustion engines or industrial boilers is one of the most urgent challenges at present due to the serious effects of N_2O not only on the ozonosphere and the greenhouse effect but also to our health [1–3]. One of the most promising methods for the depletion of N_2O is the development of new catalysts that work to decompose N_2O with reducing agents such as CO and hydrocarbons [4]. Previously, we have reported that Ag^+ ion catalysts anchored within zeolite cavities show high photocatalytic activity for the direct decomposition of N_2O into N_2 and O_2 [5].

On the other hand, metal diimine complexes are of great interest since they have shown high photocatalytic activity for CO_2 reduction [6], the photoevolution of H_2 from aqueous solution [7], and the photocatalytic oxidation of sulfur containing compounds [8]. The photocatalytic selective oxidation of various hydrocarbons by photo-stable dimer-iron(III) bisporphine complexes has been reported to proceed under visible light irradiation with high turnover numbers and selectivity [9]. Furthermore, copper Schiff base complexes encapsulated within Y-zeolites as well as copper complexes anchored in mesoporous silica MCM-41 matrices have been reported to show excellent catalytic activity for the hydroxylation of phenol or 1-naphthol [10] and the epoxidation of olefins by *tert*-BuOOH [11], respectively. Recently, a platinum(II) complex loaded into the channels of ordered mesoporous silica, SBA-15, was also found to be stable and to induce the oxidation of olefins more efficiently than the platinum(II) complex in solution [12].

It is known that 2,2′-bipyridine (bpy) is a typical flexible bidentate chelating ligand for transitional metal ions leading to complexes that are promising for such applications as solar energy conversion and catalytic reactions [13]. The present work deals with the successful covalent immobilization of bipyridine derivatives on the surface of the mesopores of MCM-41 and their further chelation with Ag^+ ions to form Ag^+ bipyridine complexes. These Ag^+

H. Chen · S. Kuranari · M. Matsuoka · M. Anpo (✉)
Department of Applied Chemistry, Graduate School of Engineering, Osaka Prefecture University, 1-1 Gakuen-cho, Naka-Ku, Sakai, Osaka 599-8531, Japan
e-mail: anpo@chem.osakafu-u.ac.jp

J. Zhang
Institute of Fine Chemicals, East China University of Science and Technology, 130 Meilong Road, Shanghai 200237, People's Republic of China

bipyridine complexes within MCM-41 were found to exhibit much higher photocatalytic activity for N_2O reduction with CO than the $Ag(bpy)_3NO_3$ complexes or Ag^+ ion catalysts supported on MCM-41. The dependence of the photocatalytic activity on the irradiation wavelength was also investigated to identify the active species for the photocatalytic reduction of N_2O with CO.

2 Experimental

MCM-41 was prepared according to procedures detailed in previous literature [14]. The as-synthesized MCM-41 was calcined in air at 823 K for 5 h for the surface modification with the bipyridine derivatives.

The preparation of the Ag bipyridine complexes anchored in the mesopores of MCM-41 is shown in Scheme 1. First, 4,4′-bis(chlorocarbonyl)-2,2′-bipyridine (**1**) was synthesized from commercially available 4,4′-dimethyl-2,2′-bipyridine (Aldrich) according to previously reported procedures [15, 16]. A solution of compound **1** (0.35 g, 1.25 mmol) in $CHCl_3$ (30 mL) was then slowly added dropwise to a stirred mixture solution of 3-aminopropyltriethyloxysilane (APTES, **2**) (0.60 mL, 2.50 mmol, 2 equiv) and triethylamine (0.54 mL, 3.75 mmol, 3 equiv) in $CHCl_3$ (20 ml) for 1 h. The resulting mixture was refluxed under nitrogen atmosphere for 1 h to obtain a 4,4′-bis(chlorocarbonyl)-2,2′-bipyridine bis-[(3-triethyloxysilylpropyl)amide (**3**) solution. Next, 0.5 g MCM-41 was suspended into the above solution and the obtained mixture was stirred overnight at room temperature (r.t.) under nitrogen atmosphere. The solution was filtered off and the solid was washed three times consecutively with $CHCl_3$, H_2O, methanol and diethyl ether. The obtained solid was then dried overnight at 323 K and finally dried again overnight under vacuum at r.t. to obtain a powder, hereby, referred to as bpy-MCM-41.

Precisely 0.2 g of bpy-MCM-41 was suspended into a stirred aqueous $Ag(NH_3)_2^+$ solution (6 mM, 40 mL) overnight and the solutions were then filtered off. The obtained solids were then washed three times with acetone and dried at 323 K overnight to obtain a powder, hereby, referred to as Ag-bpy-MCM-41. For comparison, $Ag(bpy)_2NO_3$ complexes were synthesized according to procedures reported in previous literature [17]. MCM-41 supported with Ag^+ ion catalysts were prepared as a reference sample by the impregnation of MCM-41 with an aqueous $Ag(NH_3)_2^+$ solution and the obtained solids were dried at 323 K overnight to obtain a powder, hereby, referred to as Ag-MCM-41.

The X-ray powder diffraction (XRD) patterns were recorded on a Shimadzu XRD-6100 diffractometer using CuK_α radiation. Elemental analyses of the C and N present in the samples were carried out using a Yanako CHN coder

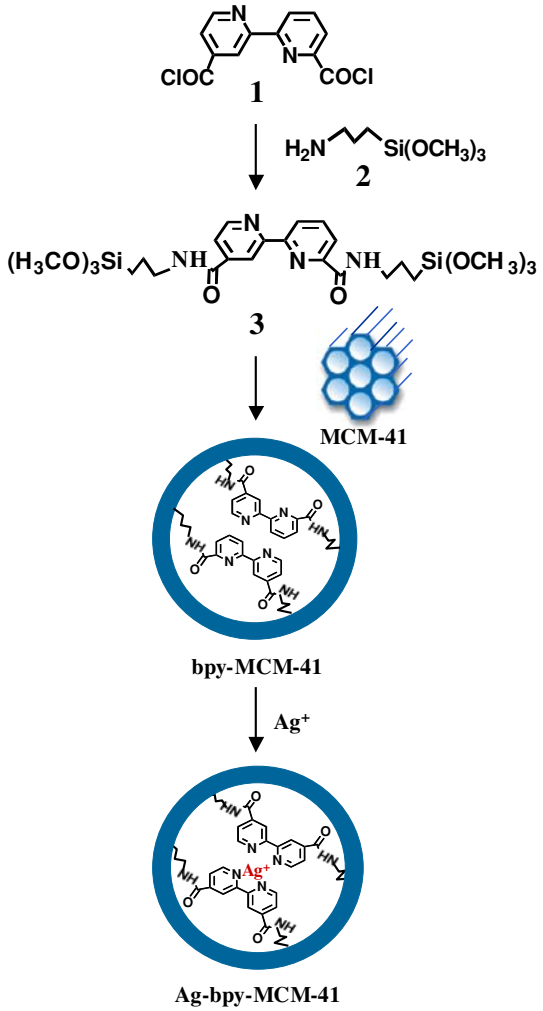

Scheme 1 The preparation of Ag^+ bipyridine complexes anchored on the surface of the mesopores of MCM-41

(MT-3) to evaluate the loading of the bipyridine derivatives. The loadings of Ag^+ ions in the obtained samples were determined as 2.74 and 2.50 wt.% for Ag-bpy-MCM-41 and Ag-MCM-41, respectively, by atomic absorption flame emission spectrophotometry (AAS, Shimadzu AA-6400F). The UV-vis reflection spectra were recorded using a double-beam digital spectrophotometer (Shimadu UV-2200A) using a $BaSO_4$ powder as reference. The FT-IR spectra were recorded with an FT-IR spectrometer (JASCO FT-IR 7300) using a TGS detector under a nominal resolution of 2 cm^{-1} and by averaging 100 scans in transmission mode. Analysis by X-ray photoelectron spectroscopy (XPS, Shimadzu ESCA-3200) was carried out to investigate the electronic state of the Ag ions. All of the quartz cells used for the in situ spectroscopic measurements were specially designed to connect with a vacuum line for thermal treatment of the samples. Prior to spectroscopic measurements and photocatalytic reactions, the samples were evacuated at 353 K for 2 h to remove

adsorbates such as H_2O. The photocatalytic reduction of N_2O with CO (20 Torr; volume ratio: 1:1) were carried out under UV light irradiation of the Ag catalysts (50 mg) with a 500 W high-pressure mercury lamp (USH-500BY, $\lambda > 200$ nm) through a water filter at 298 K. The products were analyzed by gas chromatography (Shimadzu GC-7A). A UV-25 filter (Toshiba, $\lambda > 250$ nm) and UV-35 filter (Toshiba, $\lambda > 350$ nm) were used to examine the effect of the irradiation wavelength on the reactions.

3 Results and Discussion

The powder XRD patterns of MCM-41 were compared with those of bpy-MCM-41 and Ag-bpy-MCM-41, as shown in Fig. 1. Three well-defined peaks in low angle range ($2° < 2\theta < 5°$) corresponding to the (100), (110), and (200) planes of MCM-41 [14], respectively, were observed for all the samples. A decrease in the intensity of the XRD peaks and a slight increase in the d_{100} value were observed for bpy-MCM-41 and Ag-bpy-MCM-41 as compared with MCM-41. The decrease in the scattering efficiency for the pores and framework of MCM-41 and an increase in the d_{100} value are attributed to the pore-filling effect [18–20], showing that bipyridine derivates as well as Ag bipyridine complexes were immobilized on the inner surface of the mesopores of MCM-41.

The successful covalent immobilization of the bipyridine derivatives and Ag bipyridine complexes were further confirmed by various spectroscopic measurements. Figure 2 shows the FT-IR spectra of Ag-bpy-MCM-41, Ag-MCM-41 and $Ag(bpy)_2NO_3$. Judging from the strong absorption band at 3,750 $\sim$ 3,300 cm^{-1} due to the surface silanols observed for Ag-MCM-41, the weak intensity of the absorption band at 3,750 $\sim$ 3,300 cm^{-1} for Ag-bpy-MCM-41 can be ascribed to the elimination of parts of the silanols of MCM-41 by their reaction with the triethyloxysilane units of the bipyridine derivatives. These results show that bipyridine derivatives were covalently immobilized on the surface of the mesopores of MCM-41. As shown in Fig. 2b, Ag-bpy-MCM-41 shows a typical FT-IR band at 1,610 $\sim$ 1,450 cm^{-1} due to the bipyridine units which can also be observed for $Ag(bpy)_2NO_3$. The presence of the stretching vibration absorption of NH (3,343 cm^{-1}), CH_2 (2,950 cm^{-1}) and CH (2,900 cm^{-1}), together with the stretching vibrations of CONH and C–N at 1,630 and 1,416 cm^{-1}, respectively, further confirms that the bipyridine derivatives are anchored on the surface of the mesopores of MCM-41. These immobilized Ag bipyridine complexes in Ag-bpy-MCM remains stable even after evacuation treatment at 453 K for 2 h, while the $Ag(bpy)_2NO_3$ complexes decomposed even at a low temperature of 428 K [21].

According to the results of elemental analyses, the molar ratio of C to N (C/N) for bpy-MCM-41 was determined at about 4.56, which is consistent with the theoretical molar ratio of the bipyridine derivatives ($C_{18}H_{20}N_4O_2$–Si(O), C/N = 4.5). The loading of the bipyridine derivates was evaluated to be 0.38 mmol/g based on elemental analysis of C since almost no organic residue can be observed for the calcined MCM-41.

Considering the surface area of the calcined MCM-41 (950 m^2/g) [14], the surface density of the bipyridine molecule can be estimated at about 0.25/nm^2. Moreover, the loading of Ag ions for Ag-bpy-MCM-41 was found to be 2.74 wt.% by AAS measurements while the molar ratio of the Ag^+ ions to bipyridine molecules was estimated at 0.67. Figure 3a shows the UV-vis spectrum of bpy-MCM-

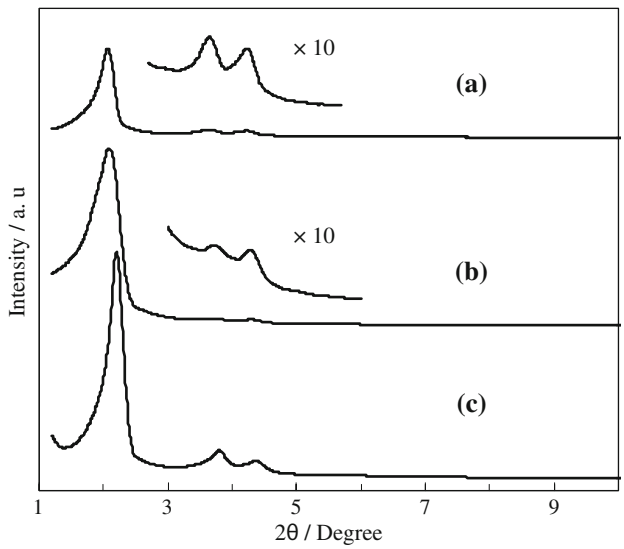

Fig. 1 Powder XRD diffraction patterns of: (**a**) Ag-bpy-MCM-41; (**b**) bpy-MCM-41; and (**c**) MCM-41

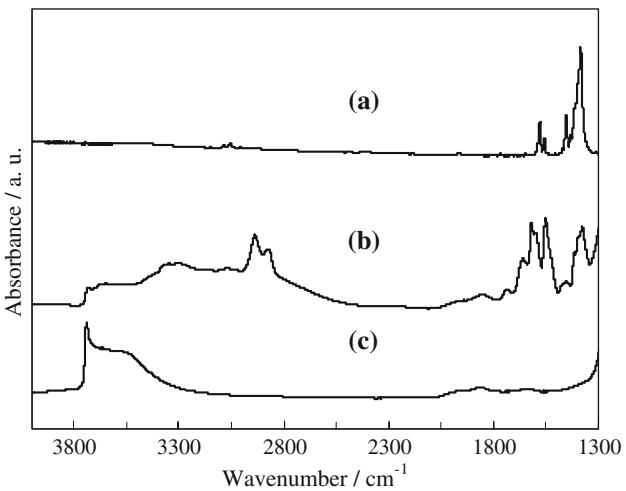

Fig. 2 FT-IR spectra of: (**a**) $[Ag(bpy)_2]NO_3$; (**b**) Ag-bpy-MCM-41; and (**c**) Ag-MCM-41. (**b**) and (**c**) were measured after evacuation at 453 K for 2 h

41. Two broad absorption bands at around 240 and 280 nm can be ascribed to the $\pi \rightarrow \pi^*$ electronic transition of the bipyridine units in the trans-planar conformation anchored in the MCM-41 channels [22]. The introduction of Ag^+ ions to bpy-MCM-41 induced an apparent red shift in the UV absorption bands. As shown in Fig. 3b, Ag-bpy-MCM-41 exhibited two broad absorption bands at around 250 and 310 nm corresponding to the $\pi \rightarrow \pi^*$ electronic transition of the bipyridine units in cisoid or cis-planar conformation [22]. This conformation transfer of the bipyridine units was attributed to the formation of Ag bipyridine complexes by the chelation of the Ag^+ ions with the bipyridine units [13]. On the other hand, Ag-MCM-41 exhibited typical broad absorption bands at around 220 nm and 430 nm due to the isolated Ag^+ ion species and aggregated Ag_n^0 clusters [23, 24], respectively [Fig. 3c], showing that the reduction and aggregation of the Ag^+ species can proceed easily on MCM-41 surfaces. The absence of a UV absorption band above 350 nm for Ag-bpy-MCM-41 suggests that the chelation of Ag^+ with the bipyridine units prevented the formation of Ag clusters even after evacuation treatment at 453 K for 2 h, in clear contrast to Ag-MCM-41.

XPS investigations were carried out to determine the chemical state of the silver species of the prepared samples, as shown in Fig. 4. Compared with the Ag $3d_{5/2}$ band of $AgNO_3$ at 370.1 eV, the Ag $3d_{5/2}$ bands of the Ag-bpy-MCM-41 and $[Ag(bpy)_2]NO_3$ complexes were observed in lower energy regions of 368.6 eV and 368.2 eV, respectively. However, both the binding energy of Ag-bpy-MCM-41 and $[Ag(bpy)_2]NO_3$ were higher than that of Ag metal (367.9 eV). These shifts in the Ag $3d_{5/2}$ bands of Ag-bpy-MCM-41 and $Ag(bpy)_2NO_3$ may be explained by the increases in the electronic density around the Ag^+ ions resulting from electron draining from the nitrogen atoms of the bipyridine units to the Ag^+ ions through their close interactions [25]. XPS spectral analysis further confirmed the formation of an Ag bipyridine complex in the mesopores of MCM-41, further supporting the results evidenced by UV-vis measurements.

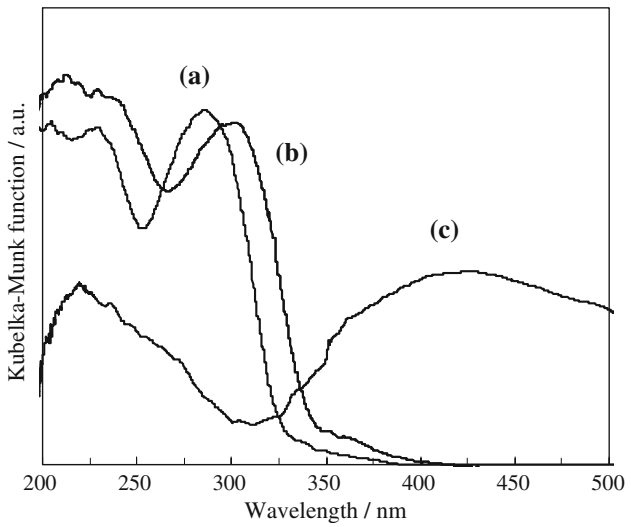

Fig. 3 UV-vis reflection spectra of: (**a**) bpy-MCM-41; (**b**) Ag-bpy-MCM-41; and (**c**) Ag-MCM-41

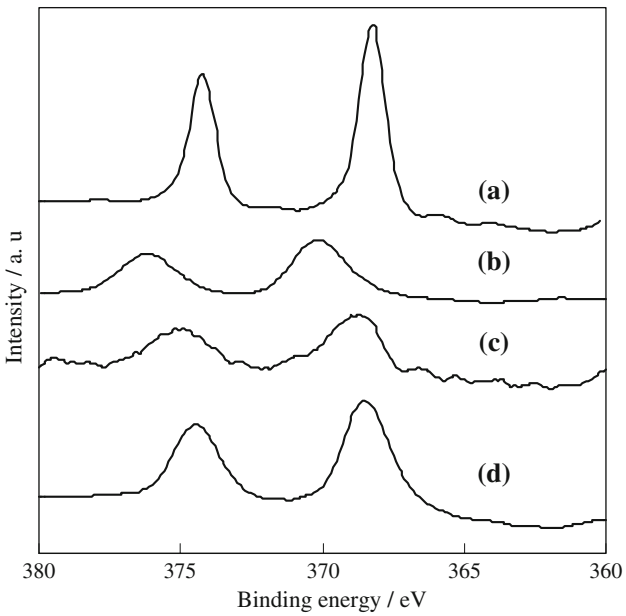

Fig. 4 XPS spectra of: (**a**) Ag metal; (**b**) $AgNO_3$; (**c**) Ag-bpy-MCM-41; and (**d**) $Ag(bpy)_2NO_3$

Figure 5 shows the photoluminescence spectra of bpy-MCM-41, Ag-bpy-MCM-41 and Ag-MCM-41 measured at 77 K. The bpy-MCM-41 catalyst exhibits a weak emission band at around 360 nm and a strong broad emission band at 430 $\sim$ 600 nm, which can be ascribed to the anchored bipyridine units on MCM-41 [26, 27]. The chelation of the Ag^+ ions with bpy-MCM-41 led to a quenching of the emission band at 430 $\sim$ 600 nm as well as a slight increase in the emission at around 360 nm for Ag-bpy-MCM-41. The increase in the photoluminescence at 360 nm can be assigned to the presence of some isolated Ag^+ ions in Ag-bpy-MCM-41, according to a previous study [28]. However, Ag-MCM-41 shows a broad emission band with peaks at 400 nm and 590 nm which can be assigned to the formation of Ag^+ oligomers in MCM-41 [29, 30]. As the photoluminescence spectra due to the Ag oligomers could not be observed in Ag-bpy-MCM-41, the presence of the bipyridine units in MCM-41 is assumed to effectively prevent the formation of Ag clusters in MCM-41.

The photocatalytic activity of Ag-bpy-MCM-41 was investigated by N_2O reduction with CO. As shown in Fig. 6, UV light irradiation of Ag-bpy-MCM-41 in the presence of N_2O and CO at 298 K led to the efficient formation of N_2 and CO_2. Moreover, under dark conditions, no reactions were observed, indicating that these reactions proceeded photocatalytically. The Ag-bpy-

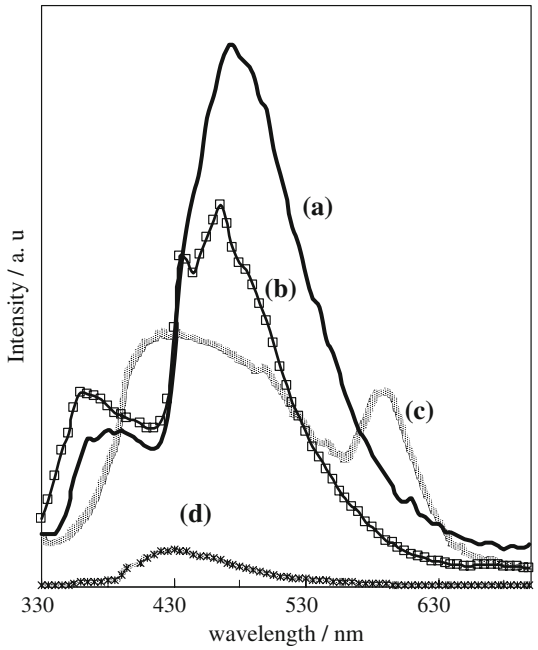

Fig. 5 Photoluminecence spectra of: (**a**) bpy-MCM-41; (**b**) Ag-bpy-MCM-41; (**c**) Ag-MCM-41; and (**d**) MCM-41. Photoluminescence spectra were measured at 77 K under excitation at 250 nm

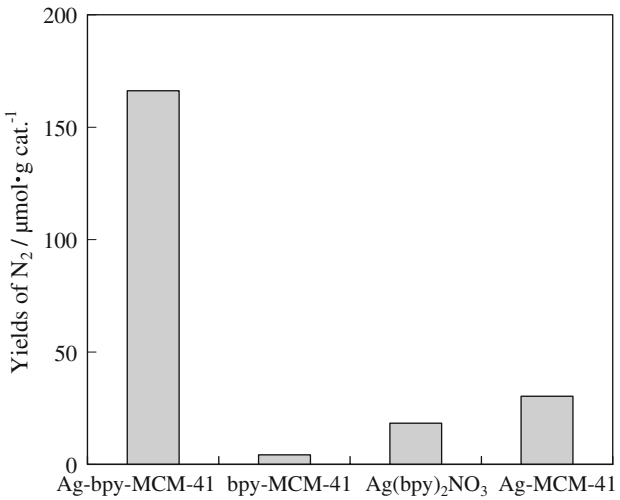

Fig. 6 The yields of N_2 for the photocatalytic reduction of N_2O with CO on Ag-bpy-MCM-41, bpy-MCM-41, $Ag(bpy)_2NO_3$, and Ag-MCM-41. Reaction time: 4 h

MCM-41 catalyst shows much higher activity than the Ag-MCM-41 catalyst and $Ag(bpy)_2NO_3$ complex, while the bpy-MCM-41 catalyst shows almost no activity, indicating that the existence of an Ag^+ species is an indispensable factor in the reaction. The effect of the irradiation wavelength on the photocatalytic activity is shown in Fig. 7. The most effective light for N_2O reduction on Ag-bpy-MCM-41 was found to lie in the wavelength range between 250 nm and 350 nm. In contrast, light

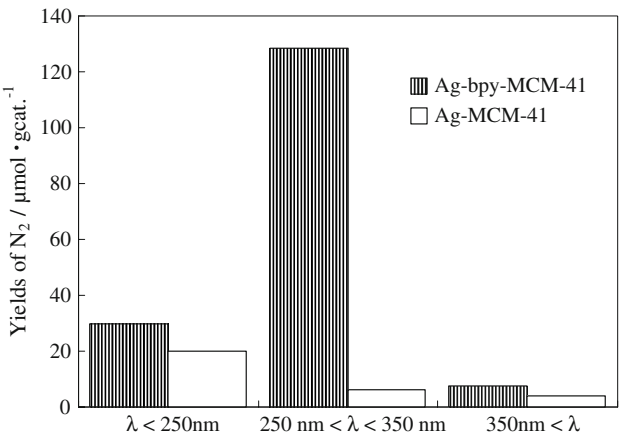

Fig. 7 The effect of the irradiation wavelength on the photocatalytic activity of Ag-bpy-MCM-41 and Ag-MCM-41

wavelengths below 250 nm were found to be most effective for the reduction on Ag-MCM-41. Considering the results of UV-vis measurements, it could be concluded that the Ag^+ bipyridine complexes anchored on the surface of the mesopores of Ag-bpy-MCM-41 catalysts, with UV absorption bands between 250 and 350 nm, play an indispensable role in the photocatalytic reduction of N_2O with CO. On the other hand, the isolated Ag^+ ions supported on MCM-41 with UV absorption bands below 250 nm contributed as the active species for the photocatalytic reduction of N_2O with CO on Ag-MCM-41.

It is known that UV light irradiation of Ag-MCM-41 can lead to an intra-ionic electronic transition of Ag^+ ions ($4d^{10} \rightarrow 4d^9 5\ s^1$) [5]. Thus, the electron transfer of the 5 s electron of the photoexcited Ag^+ into the antibonding molecular orbital (LUMO) of N_2O is considered to initiate the decomposition of N_2O to produce N_2 and an $O^-_{(ads)}$ species adsorbed on the catalyst surface (Eq. 1) [31]. The further reaction of CO with the $O^-_{(ads)}$ species leads to the formation of CO_2 and releases electrons which can drain to the Ag ions for a regeneration of the active sites (Eq. 2).

$$N_2O + e^- \rightarrow N_2 + O^-_{(ads)} \quad (1)$$

$$O^-_{(ads)} + CO \rightarrow CO_2 + e^- \quad (2)$$

Though irradiation between 250 and 350 nm can induce the $\pi \rightarrow \pi^*$ electronic transition of the bipyridine units, bpy-MCM-41 shows almost no photocatalytic activity for the reduction of N_2O with CO. These results mean that the bipyridine units themselves show no reactivity for the photocatalytic reaction even under light irradiation. In the photocatalytic reduction of N_2O with CO on Ag-bpy-MCM-41, the reaction is assumed to be initiated by the electron transfer of the 5 s electron for the photoexcited Ag^+ into N_2O. The bipyridine units present in Ag-bpy-MCM-41 are assumed to act as a photosensitizer, and electron transfers from the excited bipyridine to the chelated Ag^+ ions causes a

promoting effect for the initiation reaction (Eq. 1) in the decomposition of N_2O and for the regeneration of the Ag^+ active sites. Finally, the electrons released after the reaction of CO with the $O^-_{(ads)}$ species (Eq. 2) flow back to regenerate the Ag^+ bipyridine complexes present in Ag-bpy-MCM-41 for this photocatalytic cycle.

4 Conclusions

Unique bpy-MCM-41 catalysts were successfully prepared by covalently anchoring 2,2-bipyridine units on the surface of the mesopores of a MCM-41 porous material. XRD, FT-IR and UV-vis investigations showed that the further introduction of Ag^+ ions onto bpy-MCM-41 led to the formation of Ag^+ bipyridine complexes inside the mesopores of MCM-41 (Ag-bpy-MCM-41) by the efficient chelation of the Ag^+ ions with the bipyridine units. These Ag^+ bipyridine complexes were found to remain stable even after evacuation at 453 K. Ag-bpy-MCM-41 exhibited no UV-vis absorption band due to the Ag clusters which are the dominant species in Ag-MCM-41 prepared by an impregnation method. Morevoer, the Ag^+ bipyridine units within MCM-41 prevented the reduction and aggregation of the Ag^+ species.

Ag-bpy-MCM-41 showed much higher photocatalytic activity than the $Ag(bpy)_2NO_3$ complexes and Ag-MCM-41 for the photocatalytic reduction of N_2O with CO. Detailed investigations on the relationship between the irradiation wavelength and photocatalytic activity revealed that the photoexcitation of the Ag^+ bipyridine complexes anchored on the mesopores of MCM-41 plays a major role in the photocatalytic reduction of N_2O with CO, while the Ag clusters formed on Ag-MCM-41 showed no activity for the reaction.

References

1. Anpo M (2000) In: Proceedings of 12th International Congress on Catalysis, Spain, Granada, p 157
2. Anpo M (2000) In: Tundo P, Anastas P (eds) Green chemistry. Oxford University Press, New York, p 1
3. Joseph HH, Matthew AS, Robert JD (2000) J Catal 190:247
4. Roy S, Marimuthu A, Hegde MS, Madras G (2007) Appl Catal B 71(1–2):23
5. Ju WS, Matsuoka M, Iino K, Yamashita H, Anpo M (2004) J Phys Chem B 108:2128
6. Tsubaki H, Sekine A, Ohashi Y, Koike K, Takeda H, Ishitani O (2005) J Am Chem Soc 127:15544
7. Hayashida N, Yamamoto T (1999) Bull Chem Soc Jpn 72:1153
8. Iliev V, Alexiev V, Bilyarska L (1999) J Mol Catal A 137:15
9. Rosenthal J, Luckett TD, Hodgkiss JM, Nocera DG (2006) J Am Chem Soc 128:6546
10. Saha PK, Dutta B, Jana S, Bera R, Saha S, Okamoto K, Koner S (2007) Polyhedron 26:563
11. Jana S, Dutta B, Bera R, Koner S (2007) Langmuir 23:2492
12. Feng K, Zhang RY, Wu LZ, Tu B, Peng ML, Zhang LP, Zhao DY, Tung CH (2006) J Am Chem Soc 128:14685
13. Moissette A, Gener I, Bremard C (2001) J Phys Chem B 105:5647
14. Mal NK, Fujiwara M, Tanaka Y, Taguchi T, Matsukata M (2003) Chem Mater 15:3385
15. Garelli N, Vierling P (1992) J Org Chem 57:3046
16. Uppadine LH, Keene FR, Beer PD (2001) J Chem Soc, Dalton Trans 14:2188
17. Srnova I, Vlckova B, Nemec I, Slouf M, Stepanek J (1999) J Mol Struct 482–483:213
18. Winkler H, Birkner A, Hagen V, Wolf I, Schmechel R, Von Seggern H, Fischer RA (1999) Adv Mater 11:1444
19. Zhang WH, Shi JL, Wang LZ, Yan DS (2000) Chem Mater 12:1408
20. Giri S, Trewyn BG, Stellmaker MP, Lin VSY (2005) Angew Chem Int Ed Engl 44:5038
21. Morgan GT, Burstall FH (1930) J Chem Soc 2594
22. Liu B, Yu WL, Pei J, Liu SY, Lai YL, Huang W (2001) Macromolecules 34:7932
23. Dai WL, Cao Y, Ren LP, Yang XL, Xu JH, Li HX, He HY, Fan KN (2004) J Catal 228:80
24. Yamamoto R, Sawayama Y, Shibahara H, Ichihashi Y, Nishiyama S, Tsuruya S (2005) J Catal 234:308
25. Sun S, Wang A (2006) React Funct Polym 66:819
26. Henry MS, Hoffman MZ (1977) J Am Chem Soc 99:5201
27. Qian G, Wang M (2002) Mater Lett 56:71
28. Anpo M, Zhang S, Mishma H, Matsuoka M, Yamashita H (1997) Catal Today 39:159
29. Kanan SM, Omary MA, Patterson HH, Matsuoka M, Anpo Masakazu (2000) J Phys Chem B 104:3507
30. Kanan SM, Kanan MC, Patterson HH (2001) J Phys Chem B 105:7508
31. Sano T, Negishi N, Mas D, Takeuchi K (2000) J Catal 194:71